

# Imaging & Dynamics for Physical & Life Sciences

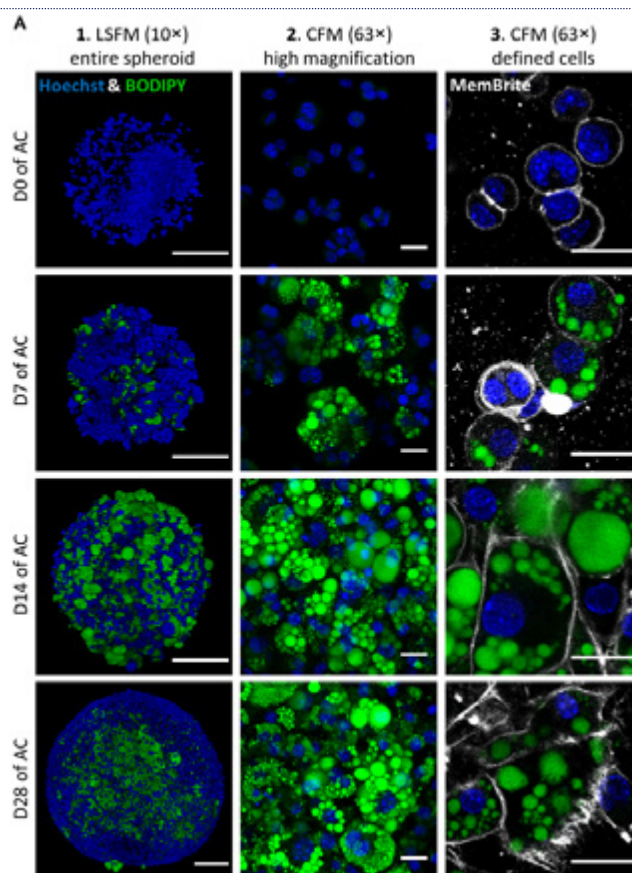
## The development of a high throughput drug-responsive model of white adipose tissue comprising adipogenic 3T3-L1 cells in a 3D matrix

**A.D. Graham, V.S. Tsancheva, T.S. Babra, X. Xue, J. Gannon, S.N. Olof** (OxSyBio Ltd, Building B27, Rutherford Appleton Laboratory, Harwell Campus, Didcot, UK)  
**R. Pandey, L.A.K. Zolkiewski, L. Bentley, R.D. Cox** (Medical Research Council Harwell Institute, Mammalian Genetics Unit, Harwell Campus, Oxfordshire, UK)  
**A. Candeo, S.W. Botchway** (Central Laser Facility, Research Complex at Harwell, STFC Rutherford Appleton Laboratory, Harwell Campus, Didcot, UK)

**A.J. Allan, L. Teboul** (Medical Research Council Harwell Institute, Mary Lyon Centre, Harwell Campus, Oxfordshire, UK)  
**K. Madi** (3Dmagination, Building B27, Rutherford Appleton Laboratory, Harwell Campus, Didcot, UK)

Adipose models have been applied to mechanistic studies of metabolic diseases (such as diabetes) and the subsequent discovery of new therapeutics. However, typical models are either insufficiently complex (2D cell cultures) or expensive and labour intensive (mice/*in vivo*). To bridge the gap between these models and to better inform pre-clinical studies, we have developed a drug-responsive 3D model of white adipose tissue (WAT). Here, spheroids ( $680 \pm 60 \mu\text{m}$ ) comprising adipogenic 3T3-L1 cells encapsulated in 3D matrix were fabricated manually on a 96 well scale. Spheroids were highly characterised for lipid morphology, selected metabolite and adipokine secretion, and gene expression; displaying significant upregulation of certain adipogenic-specific genes compared with a 2D model. Furthermore, induction of lipolysis and promotion of lipogenesis in spheroids could be triggered by exposure to 8-br-cAMP and oleic acid respectively. Metabolic and high content imaging data of spheroids exposed to an adipose-targeting drug, rosiglitazone, resulted in dose-responsive behaviour. Thus, our 3D WAT model has potential as a powerful scalable tool for compound screening and for investigating adipose biology.

Reproduced from Alexander D Graham et al. 2020 *Biofabrication* 12 015018, under the terms of the Creative Commons Attribution 3.0 licence. doi:10.1088/1758-5090/ab56fe



**Lipid morphology of 3T3-L1 spheroids exposed to adipogenic cocktail. (A)** A matrix of image projections depicting the change of lipid morphology within singlet spheroids over 28 days of adipogenic cocktail (AC) exposure. Spheroids were stained for nuclei (Hoechst 33342, blue), lipid droplets (BODIPY 493/503, green) and the cell membrane (MemBrite, white). Fluorescence z-stack micrographs were acquired by either light sheet fluorescence microscopy (LSFM, (A1),  $200 \mu\text{m}$  scale bar) or confocal fluorescence microscopy (CFM, (A2) and (A3),  $25 \mu\text{m}$  scale bars).

Contact: S.N. Olof (sam.nicholas.olofof@gmail.com)  
 R.D. Cox (r.cox@har.mrc.ac.uk)

## The Rho family GEF FARP2 is activated by aPKC $\zeta$ to control tight junction formation and polarity

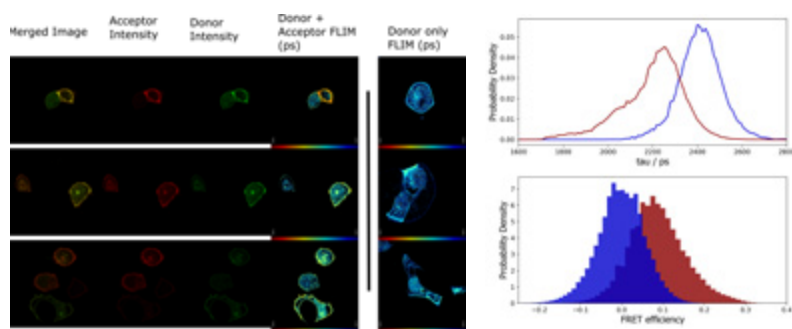
**A. Elbediwy, B.J. Thompson** (Epithelial Biology Laboratory, Francis Crick Institute, London, UK)  
**Y. Zhang, M. Cobbaut, P. Riou, R.S. Tan** (Protein Phosphorylation Laboratory, Francis Crick Institute, London, UK)  
**S.K. Roberts, C. Tynan, M.L. Martin-Fernandez** (Central Laser Facility, STFC Rutherford Appleton Laboratory, Harwell Campus, Didcot, UK)

**R. George, S. Kjaer** (Structural Biology Team, Francis Crick Institute, London, UK)  
**N.Q. McDonald** (Signalling and Structural Biology Laboratory, Francis Crick Institute, London, UK)  
**P.J. Parker** (Protein Phosphorylation Laboratory, Francis Crick Institute, London, UK; School of Cancer and Pharmaceutical Sciences, King's College London, UK)

The elaboration of polarity is central to organismal development and to the maintenance of functional epithelia. Among the controls determining polarity are the PAR proteins, PAR6, aPKC $\zeta$  and PAR3, regulating both known and unknown effectors. Here, we identify FARP2 as a 'RIPR' motif-dependent partner and substrate of aPKC $\zeta$  that is required for efficient polarisation and junction formation. Binding is conferred by a FERM/FA domain–kinase domain interaction and detachment promoted by aPKC $\zeta$ -dependent phosphorylation. FARP2 is shown

to promote GTP loading of Cdc42, which is consistent with it being involved in upstream regulation of the polarising PAR6–aPKC $\zeta$  complex. However, we show that aPKC $\zeta$  acts to promote the localised activity of FARP2 through phosphorylation. We conclude that this aPKC $\zeta$ –FARP2 complex formation acts as a positive feedback control to drive polarisation through aPKC $\zeta$  and other Cdc42 effectors.

Reproduced from Elbediwy A, Zhang Y, Cobbaut M, et al. *J Cell Sci*. 2019;132(8):jcs223743, published by The Company of Biologists Ltd, under the terms of the Creative Commons Attribution License 4.0. doi: 10.1242/jcs.223743



GFP-PKC $\zeta$  and FLAG-FARP2 were coexpressed in HCT116 cells. GFP lifetime was monitored at 488nm in the absence (indicated Donor only) or presence of Anti-HA Alexa 647 as exemplified in the upper panels. Lifetime values of doubly transfected cells were captured and quantified. Lifetimes ( $\tau$ ) in picoseconds (ps) and the derived FRET efficiencies are shown for the donor only (blue) and donor-acceptor (umber) analyses

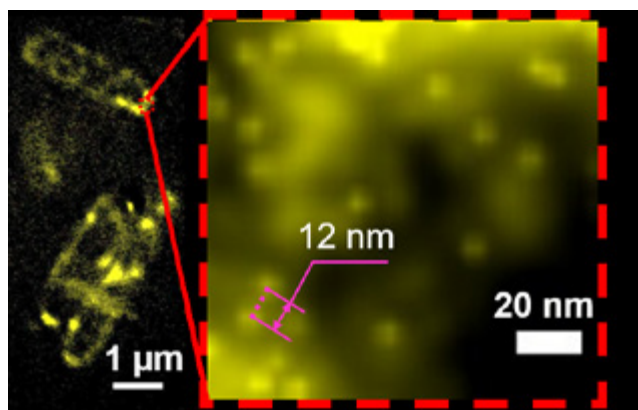
Contact: S.K. Roberts (selene.roberts@stfc.ac.uk) P.J. Parker (peter.parker@crick.ac.uk)

## Solid immersion microscopy images cells under cryogenic conditions with 12 nm resolution

**L. Wang, B. Bateman, L.C. Zanetti-Domingues, A.N. Moores, S. Astbury, C. Spindloe, S.R. Needham, D.J. Rolfe, D.T. Clarke, M.L. Martin-Fernandez** (Central Laser Facility, Research Complex at Harwell, STFC Rutherford Appleton Laboratory, Harwell Campus, Didcot, UK)

**M.C. Darrow** (Diamond Light Source, Harwell Science & Innovation Campus, Didcot, UK)  
**M. Romano, K. Beis** (Department of Life Sciences, Imperial College London, UK; Research Complex at Harwell, STFC Rutherford Appleton Laboratory, Harwell Campus, Didcot, UK)

Super-resolution fluorescence microscopy plays a crucial role in our understanding of cell structure and function by reporting cellular ultrastructure with 20–30 nm resolution. However, this resolution is insufficient to image macromolecular machinery at work. A path to improve resolution is to image under cryogenic conditions. This substantially increases the brightness of most fluorophores and preserves native ultrastructure much better than chemical fixation. Cryogenic conditions are, however, underutilised because of the lack of compatible high numerical aperture objectives. Here, using a low-cost super-hemispherical solid immersion lens (superSIL) and a basic set-up we achieve 12 nm resolution under cryogenic conditions, to our knowledge the best yet attained in cells using simple set-ups and/or commercial systems. By also allowing multicolour imaging, and by paving the way to total-internal-reflection fluorescence imaging of mammalian cells under cryogenic conditions, superSIL microscopy opens a straightforward route to achieve unmatched resolution on bacterial and mammalian cell samples.



Cryogenic solid immersion localisation microscopy imaging of *E. coli* cells. On the left hand side, it is shown the image of a field of *E. coli* cells in which ATP-binding cassette (ABC) transporter protein PH1735 were fused with EGFP. On the right hand side, it is shown the enlarged image of the region indicated by the red dashed border box. Two 12 nm apart PH1735 proteins can be clearly resolved.

Reproduced from Wang, L., Bateman, B., Zanetti-Domingues, L.C. et al. *Commun Biol* 2, 74 (2019) under the terms of the Creative Commons CC BY License. doi: org/10.1038/s42003-019-0317-6 © Springer Nature 2019

Contact: M.L. Martin-Fernandez (marisa.martin-fernandez@stfc.ac.uk)

## A signal motif retains Arabidopsis ER- $\alpha$ -mannosidase I in the cis-Golgi and prevents enhanced glycoprotein ERAD

J. Schoberer, J. König, C. Veit, U. Vavra, E. Liebminger, R. Strasser (Department of Applied Genetics and Cell Biology, University of Natural Resources and Life Sciences, Vienna, Austria)  
 S.W. Botchway (Central Laser Facility, Research Complex at Harwell, STFC Rutherford Appleton Laboratory, Harwell Campus, Didcot, UK)

F. Altmann (Department of Chemistry, University of Natural Resources and Life Sciences, Vienna, Austria)

V. Kriechbaumer, C. Hawes (Department of Biological and Medical Sciences, Faculty of Health and Life Sciences, Oxford Brookes University, UK)

The Arabidopsis ER- $\alpha$ -mannosidase I (MNS3) generates an oligomannosidic N-glycan structure that is characteristically found on ER-resident glycoproteins. The enzyme itself has so far not been detected in the ER. Here, evidence is provided indicating plants MNS3 exclusively resides in the Golgi apparatus. Notably, MNS3 remains on dispersed punctate structures when subjected to different approaches that commonly result in the relocation of Golgi enzymes to the ER. Responsible for this rare behaviour is an amino acid

signal motif (LPYS) within the cytoplasmic tail of MNS3 that acts as a specific Golgi retention signal. The physiological importance of the very specific MNS3 localization is demonstrated.

Reproduced from Schoberer, J., König, J., Veit, L. et al. Nat Commun 10, 3701 (2019), under the terms of the Creative Commons Attribution 4.0 International License. doi: 10.1038/s41467-019-11686-9

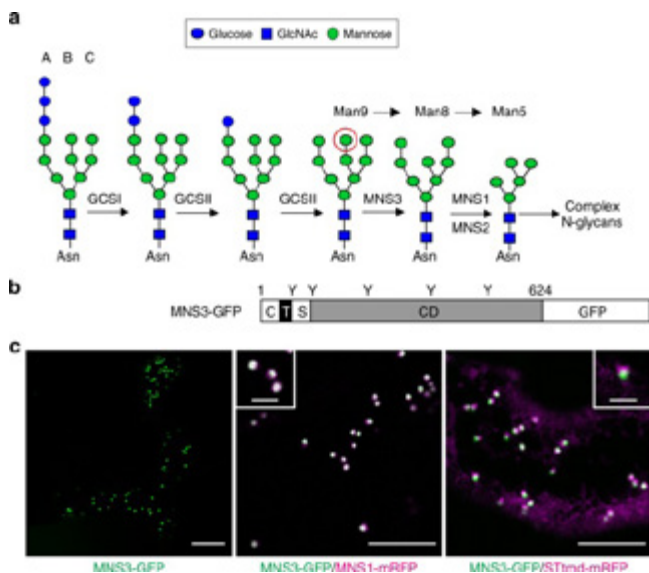


Figure 1: Arabidopsis MNS3 is a Golgi-resident protein. (a) Early steps of N-glycan processing in *A. thaliana* are shown. Confocal images show *N. benthamiana* leaf epidermal cells transiently expressing MNS3-GFP (green) alone (scale bar = 20  $\mu$ m) and in combination with the cis/medial-Golgi protein MNS1-mRFP (magenta, scale bar = 5  $\mu$ m) or the medial/trans-Golgi marker STmd-mRFP (magenta, scale bar = 5  $\mu$ m). The insets show a higher magnification of individual dual-colored Golgi stacks (scale bar = 2  $\mu$ m). Images were acquired two days post infiltration (dpi).

Contact: S. Botchway (stan.botchway@stfc.ac.uk)

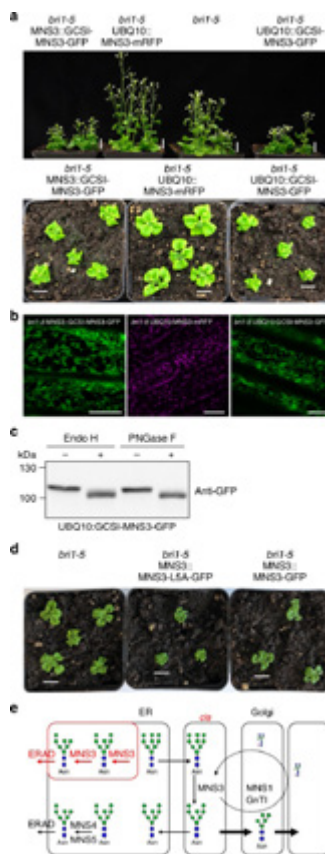


Figure 2: ER retention of MNS3 enhances the *bri1-5* phenotype. (a) Phenotype of Arabidopsis *bri1-5* and transgenic *bri1-5* plants. Images of 5-week-old (upper panel) or 26-day-old (lower panel) soil-grown plants are shown. Scale bars = 1 cm. (b) Confocal images of transgenic *bri1-5* plants expressing either MNS3::GCSI-MNS3-GFP (green), UBQ10::MNS3-mRFP (magenta), or UBQ10::GCSI-MNS3-GFP (green). Scale bar = 15  $\mu$ m. (c) Crude protein extracts from leaves of *N. benthamiana* wild-type plants transiently expressing UBQ10::GCSI-MNS3-GFP (d) Phenotype of *bri1-5* and transgenic *bri1-5* plants expressing either MNS3::MNS3-L5A-GFP or MNS3::MNS3-GFP. Images of 22-day-old soil-grown plants are shown. Scale bars = 1 cm. (e) Proposed model for MNS3-catalyzed mannose trimming. See doi: 10.1038/s41467-019-11686-9 for full details of figures

## Candidalysin activates innate epithelial immune responses via epidermal growth factor receptor

**J. Ho, X. Yang, S.-A. Nikou, A. Donkin, N.O. Ponde, J.P. Richardson, C. Murciano, D.L. Moyes, J.R. Naglik** (Centre for Host-Microbiome Interactions, Faculty of Dental, Oral and Craniofacial Sciences, King's College London, UK)

**N. Kichik** (Centre for Host-Microbiome Interactions, Faculty of Dental, Oral and Craniofacial Sciences, King's College London, UK; Department of Life Sciences, Imperial College London, UK)

**R.L. Gratacap, L.S. Archambault, C.P. Zwirner** (Department of Molecular & Biomedical Science, University of Maine, Orono, USA)

**R.T. Wheeler** (Department of Molecular & Biomedical Science, University of Maine, Orono, USA; Graduate School of Biomedical Sciences and Engineering, University of Maine, Orono, USA)

**R. Henley-Smith, S. Thavaraj** (Centre for Oral, Clinical & Translational Science, Faculty of Dental, Oral and Craniofacial Sciences, King's College London, UK)

**C. Tynan** (Central Laser Facility, Research Complex at Harwell, STFC Rutherford Appleton Laboratory, Harwell Campus, Didcot, UK)

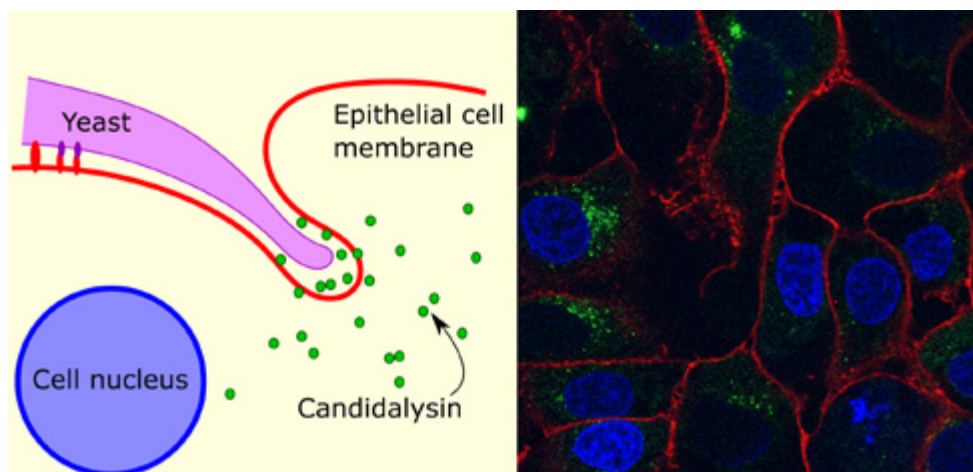
**S.L. Gaffen** (Division of Rheumatology and Clinical Immunology, University of Pittsburgh, USA)

**B. Hube** (Department of Microbial Pathogenicity Mechanisms, Leibniz Institute for Natural Product Research and Infection Biology, Hans Knöll Institute, Jena, Germany; Friedrich Schiller University, Jena, Germany)

*Candida albicans* is a fungal pathobiont, able to cause epithelial cell damage and immune activation. These functions have been attributed to its secreted toxin, candidalysin, though the molecular mechanisms are poorly understood. Here, we identify epidermal growth factor receptor (EGFR) as a critical component of candidalysin-triggered immune responses. We find that both *C. albicans* and candidalysin activate human epithelial EGFR receptors and candidalysin-deficient fungal mutants poorly induce EGFR phosphorylation during murine oropharyngeal candidiasis. Furthermore, inhibition of EGFR impairs candidalysin-triggered MAPK signalling and release of neutrophil activating chemokines in vitro, and diminishes

neutrophil recruitment, causing significant mortality in an EGFR-inhibited zebrafish swimbladder model of infection. Investigation into the mechanism of EGFR activation revealed the requirement of matrix metalloproteinases (MMPs), EGFR ligands and calcium. We thus identify a PAMP-independent mechanism of immune stimulation and highlight candidalysin and EGFR signalling components as potential targets for prophylactic and therapeutic intervention of mucosal candidiasis.

Reproduced from Ho, J., Yang, X., Nikou, S. et al. *Nat Commun* 10, 2297 (2019), under the terms of the Creative Commons Attribution License 4.0. doi:10.1038/s41467-019-09915-2



Candidalysin is a recently discovered toxin secreted by *Candida albicans* during yeast infection of human epithelial cells. The confocal microscope image on the right demonstrates how the OCTOPUS facility was used to image purified, fluorescently labelled candidalysin (coloured green) entering cultured cells (cell membranes are red, cell nuclei are blue) in order to study the mechanism of candidalysin triggered immune responses.

Contact: J. Ho (jemima.ho@kcl.ac.uk)  
J.R. Naglik (Julian.naglik@kcl.ac.uk)

## The cell wall regulates dynamics and size of plasma-membrane nanodomains in *Arabidopsis*

J.F. McKenna, A.F. Tolmie, C. Hawes, J. Runions (Department of Biological and Medical Sciences, Oxford Brookes University, UK)

D.J. Rolfe, S.E.D. Webb, S.W. Botchway, M.L. Martin-Fernandez (Central Laser Facility, Research Complex at Harwell, STFC Rutherford Appleton Laboratory, Didcot, UK)

Plant plasma-membrane (PM) proteins are involved in several vital processes, such as detection of pathogens, solute transport, and cellular signalling. For these proteins to function effectively there needs to be structure within the PM allowing, for example, proteins in the same signalling cascade to be spatially organized. Here we demonstrate that several proteins with divergent functions are located in clusters of differing size in the membrane using subdiffraction-limited Airyscan and Total Internal Reflection Fluorescence (TIRF) imaging. Single particle tracking (SPT) microscopy and analysis conducted at the OCTOPUS facility reveals that these proteins move at different rates within the

membrane. Actin and microtubule cytoskeletons appear to significantly regulate the mobility of one of these proteins (the pathogen receptor FLS2) and we further demonstrate that the cell wall is critical for the regulation of cluster size by quantifying single particle dynamics of proteins with key roles in morphogenesis (PIN3) and pathogen perception (FLS2). We propose a model in which the cell wall and cytoskeleton are pivotal for regulation of protein cluster size and dynamics, thereby contributing to the formation and functionality of membrane nanodomains.

Reproduced from McKenna JF, Rolfe DJ, Webb SED, et al. *Proc Natl Acad Sci U S A*. 2019;116(26):12857-12862, under the terms of the Creative Commons Attribution License 4.0 (CC BY). doi:10.1073/pnas.1819077116

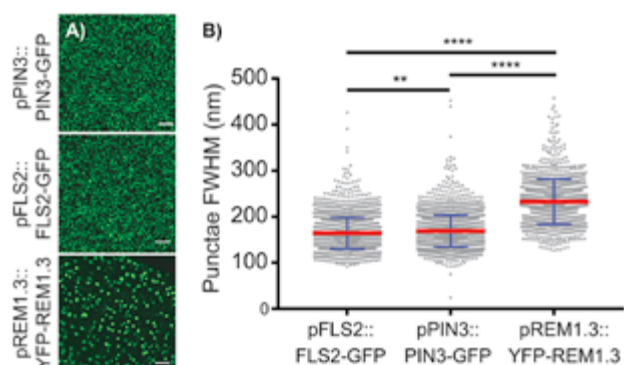


Figure 1: Zeiss Airyscan and TIRF imaging approaches were used to visualise single proteins labelled with GFP (green dots) in the plasma membrane of plant cells (A). Different membrane proteins exist in membrane microdomains of different sizes (B). The smallest of these microdomains, that of the protein PIN3-GFP, a hormone receptor, were approximately 160 nm in diameter. This is well below the theoretical limit for imaging by light microscopy and demonstrates the utility of these new super-resolution techniques.

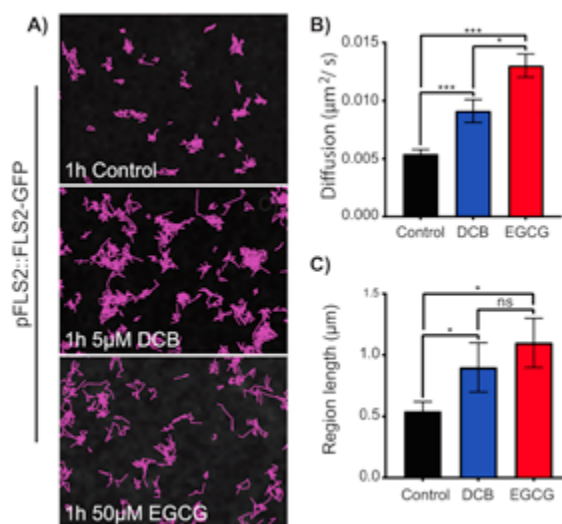


Figure 2: Timelapse imaging of the membrane protein microdomains described in Figure 1. The FLS2-GFP protein, a plant receptor that acts in the defense against pathogen attack pathway, moves laterally within the plane of the plasma membrane (pink tracks in (A)). The rate of diffusive movement of this protein and the size of the region in which it moves were calculated using SPT analysis techniques (B). Treatment of cells with chemicals that alter properties of the cell wall (DCB and EGCG) caused FLS2-GFP to move faster and increased the size of the membrane region within which it diffuses. This demonstrates the role of the cell wall in spatially regulating the distribution of defensive proteins. They are not distributed randomly but, rather, occur as discretely separated units to maximise membrane coverage.

Contact: J. Runions (jrunions@brookes.ac.uk)

## Determination of the refractive index of insoluble organic extracts from atmospheric aerosol over the visible wavelength range using optical tweezers

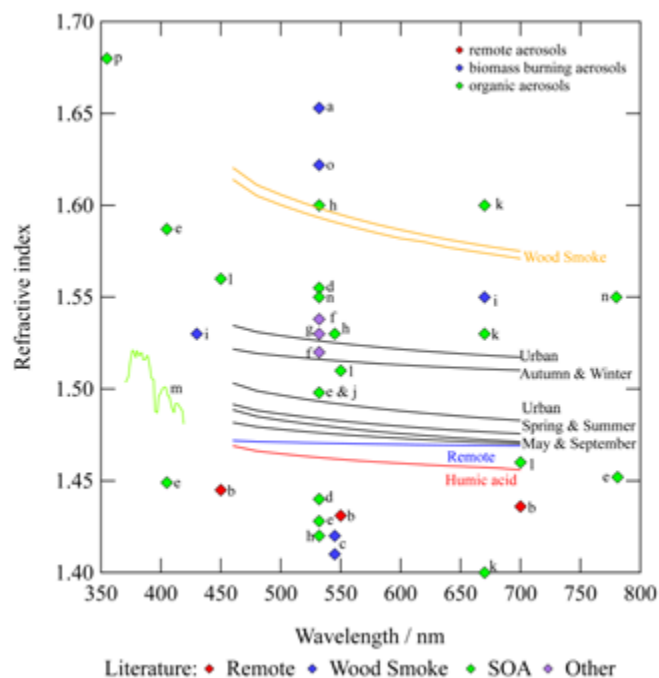
**R.H. Shepherd** (Department of Earth Sciences, Royal Holloway University of London, Egham, UK; Central Laser Facility, Research Complex at Harwell, STFC Rutherford Appleton Laboratory, Harwell Campus, Didcot, UK)  
**M.D. King** (Department of Earth Sciences, Royal Holloway University of London, Egham, UK)

**A.A. Marks, N. Brough** (British Antarctic Survey, High Cross, Cambridge, UK)  
**A.D. Ward** (Central Laser Facility, Research Complex at Harwell, STFC Rutherford Appleton Laboratory, Harwell Campus, Didcot, UK)

Atmospheric aerosol can contain a complex mixture of chemical compounds with a wide variety of physiochemical properties. The presence of organic material may alter the physical, chemical, and optical properties of cloud droplets or aerosol particles. Laser levitation of micro-droplets in air when combined with Mie spectroscopy provides a new technique to determine the refractive index of insoluble organic material extracted from atmospheric aerosol samples. The refractive index of the insoluble organic extracts was shown to follow a Cauchy equation between 460 nm and 700 nm for organic aerosol extracts collected from urban (London) and remote (Antarctica) locations. In general, the refractive index of aerosol material was found to increase from remote Antarctic summer ( $n_D = 1.470$ ) to an urban summer ( $n_D = 1.478$ ) to an urban autumn ( $n_D = 1.522$ ) to woodsmoke ( $n_D = 1.584$ ). The measured values of refractive

index compare well with previous monochromatic or small wavelength range measurements of refractive index.

Aerosol optical absorption is characterised by an Ångström exponent which defines the optical thickness of an aerosol with respect to wavelength. Mie spectra were used to determine the Ångström exponent of woodsmoke and humic acid aerosol as the spectral intensity decreases as absorption increases. Finally, a radiative-transfer calculation of the top-of-the-atmosphere albedo was applied to model an atmosphere containing a 3 km thick layer of aerosol comprising pure water, pure insoluble organic aerosol, or an aerosol consisting of an aqueous core with an insoluble organic shell. The calculation demonstrated that the top-of-the-atmosphere albedo increases by 0.01 to 0.03 for core-shell organic particles relative to water particles of the same size.



*Refractive index dispersions for urban, remote, and woodsmoke atmospheric aerosol extracts and humic acid aerosol, compared to refractive index values from the literature. A sample from literature studies that investigated aerosols from remote locations (red), biomass burning (blue) and organic aerosols (green and purple)*

Reproduced from R.H. Shepherd, M.D. King, A.A. Marks, N. Brough, A.D. Ward, *Atmos. Chem. Phys.*, 18, 5235–5252, 2018, under the terms of the Creative Commons Attribution 4.0 License. doi.org/10.5194/acp-18-5235-2018

Contact: M.D. King (m.king@rhul.ac.uk)  
 A.D. Ward (andy.ward@stfc.ac.uk)

## The architecture of EGFR's basal complexes reveals autoinhibition mechanisms in dimers and oligomers

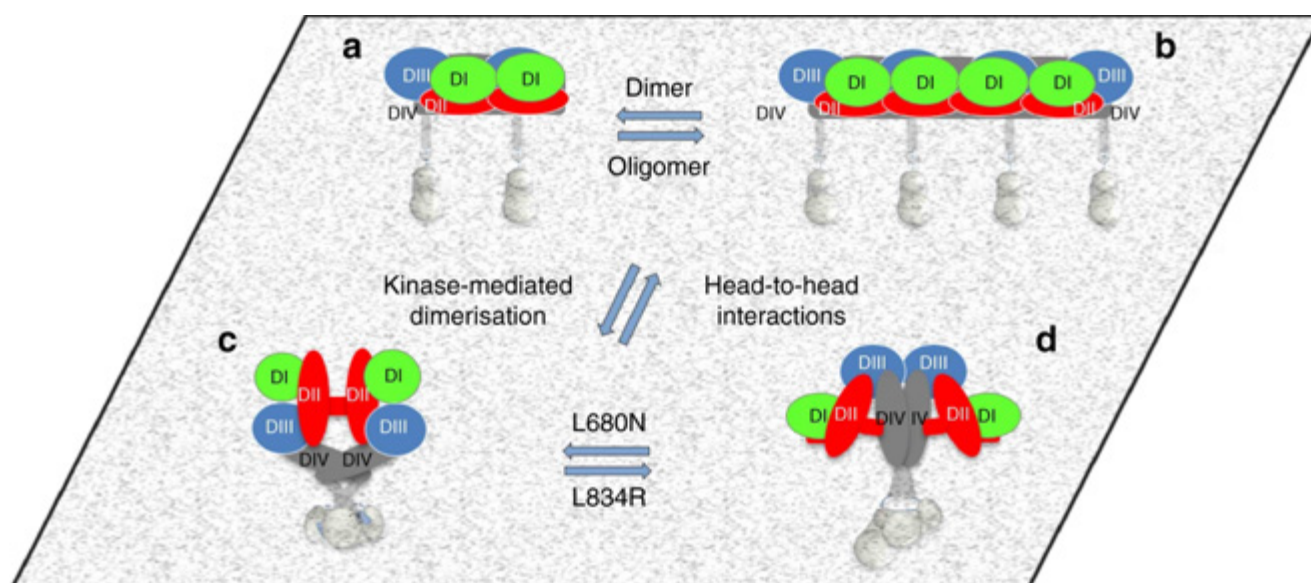
**L.C. Zanetti-Domingues, D. Korovesis, S.R. Needham, C.J. Tynan, S.K. Roberts, D.T. Clarke, D.J. Rolfe, M.L. Martin-Fernandez** (Central Laser Facility, Research Complex at Harwell, STFC Rutherford Appleton Laboratory, Harwell Oxford, Didcot, UK)  
**S. Sagawa, Y. Shan** (D.E. Shaw Research, New York, USA)  
**D.E. Shaw** (D.E. Shaw Research, New York, USA; Department of Biochemistry & Molecular Biophysics, Columbia University, New York, USA)  
**A. Kuzmanic, F.L. Gervasio** (Department of Chemistry, Faculty of Maths & Physical Sciences, University College London, UK)  
**E. Ortiz-Zapater, G. Santis** (Peter Gore Department of Immunobiology, School of Immunology & Microbial Sciences, Kings College London, UK)

**P. Jain, P.M.P. van Bergen en Henegouwen** (Division of Cell Biology, Science faculty, Department of Biology, Utrecht University, The Netherlands)  
**R.C. Roovers** (Merus, LSI, Utrecht, The Netherlands)  
**A. Lajevardipour, A.H.A. Clayton** (Centre for Micro-Photonics, Faculty of Science, Engineering & Technology, Swinburne University of Technology, Hawthorn, Australia)  
**P.J. Parker** (Protein Phosphorylation Laboratory, The Francis Crick Institute, London, UK; School of Cancer & Pharmaceutical Sciences, King's College London, UK)

Our current understanding of epidermal growth factor receptor (EGFR) autoinhibition is based on X-ray structural data of monomer and dimer receptor fragments, and does not explain how mutations achieve ligand-independent phosphorylation. Using a repertoire of imaging technologies and simulations, we reveal an extracellular head-to-head interaction through which ligand-free receptor polymer chains of various lengths assemble. The architecture of the head-to-head interaction prevents kinase-mediated dimerisation. The latter, afforded by mutation or intracellular treatments, splits the autoinhibited head-to-head polymers to form stalk-to-stalk flexible non-extended dimers structurally coupled across the plasma membrane to active asymmetric tyrosine kinase

dimers, and extended dimers coupled to inactive symmetric kinase dimers. Contrary to the previously proposed main autoinhibitory function of the inactive symmetric kinase dimer, our data suggest that only dysregulated species bear populations of symmetric and asymmetric kinase dimers that coexist in equilibrium at the plasma membrane under the modulation of the C-terminal domain.

Reproduced from Zanetti-Domingues, L.C., Korovesis, D., Needham, S.R. et al, *Nat Commun* 9, 4325 (2018), under the terms of the Creative Commons Attribution 4.0 License. <https://doi.org/10.1038/s41467-018-06632-0>



Cartoon models of ligand-free EGFR species on the cell surface. *a, b* Autoinhibited ligand-free receptors form a dimers and *b* larger oligomers via extracellular head-to-head interactions. Within head-to-head dimers and oligomers the ICMs remain as non-interacting units. *c, d* Kinase-mediated receptor dimerisation outcompetes head-to-head interactions to form two types of receptor dimers that typically coexist in equilibrium (bearing aTKD and sTKD dimer configurations). Head-to-head dimers and oligomers are disrupted by kinase-mediated dimerisation independently of whether the driver mutation and/or

treatment is activating or not. The ECM architecture of one dimer type is consistent with a back-to-back dimer and structurally coupled to an sTKD dimer<sub>6,22</sub> (*c*). The ECM architecture of the other is consistent with a stalk-to-stalk dimer and structurally coupled via an N-terminal TM crossing to the aTKD dimer<sub>40</sub> (*d*). The L680N kinase domain mutation shifts the equilibrium toward the dimer population bearing sTKD dimers while L834R shifts the equilibrium towards the dimer population bearing the aTKD dimer. For all panels, DI is in green, DII in red, DIII in blue, DIV, TMD and JMD in grey, TKD in silver

Contact: M.L. Martin-Fernandez  
 (marisa.martin-fernandez@stfc.ac.uk)

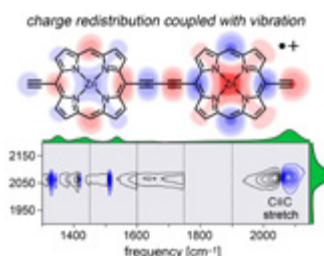
## Mechanisms of IR Amplification in Radical Cation Polarons

G.M. Greetham, I.V. Sazanovich, P.M. Donaldson, M. Towrie, A.W. Parker (Central Laser Facility, Research Complex at Harwell, STFC Rutherford Appleton Laboratory, Harwell Campus, Didcot, UK)

Break down of the Born-Oppenheimer approximation is caused by mixing of electronic and vibrational transitions in the radical cations of some conjugated polymers, resulting in intense vibrational bands known as *infrared active vibrations* (IRAVs). We have investigated the mechanism of this amplification. Spectroelectrochemical time-resolved infrared (TRIR) and two-dimensional infrared (2D-IR) spectroscopies were used to investigate the radical cations of two butadiyne-linked porphyrin oligomers: a linear dimer and a cyclic hexamer. The 2D-IR spectra reveal strong coupling between all the IRAVs and the electronic  $\pi$ - $\pi^*$  polaron band. Intramolecular vibrational energy redistribution (IVR) and vibrational relaxation occur within  $\sim 0.1$ – $7$  ps. TRIR spectra show that the transient ground state bleach (GSB) and excited state absorption (ESA) signals have anisotropies of  $0.31 \pm 0.07$  and  $0.08 \pm 0.04$  for the linear dimer and cyclic hexamer cations, respectively. The small TRIR anisotropy for the cyclic hexamer radical cation indicates that the vibrationally excited polaron migrates round the nanoring on a time scale faster than the measurement, i.e. within 0.5 ps, at 298 K. Density functional

W.J. Kendrick, M. Jirásek, M.D. Peeks, H.L. Anderson (Department of Chemistry, University of Oxford, UK)

theory (DFT) calculations qualitatively reproduce the IRAVs, and show how specific vibrational modes cause redistribution of the singly occupied molecular orbital (SOMO), amplifying the oscillator strength. These results show that IRAVs originate from the strong coupling of charge redistribution to nuclear motion, and from the similar energies of electronic and vibrational transitions.



Calculated distribution of the SOMO of the porphyrin dimer radical cation distorted by the triple bond stretch vibration. (below) 2D-IR spectra of this radical cation at 400 fs delay, with pump (FWHM  $\sim 80$   $\text{cm}^{-1}$ ) centred at  $2080$   $\text{cm}^{-1}$ . Black solid and blue dashed contour lines correspond to positive (ESA) and negative (GSB) signals, respectively.

Contact: H.L. Anderson ([harry.anderson@chem.ox.ac.uk](mailto:harry.anderson@chem.ox.ac.uk))

## Influence of zeolite topology in Catalytic Fast Pyrolysis of Biomass: a Kerr-gated Raman study using model compounds

E. Campbell, I. Lezcano-Gonzalez, A.M. Beale (Department of Chemistry, University College London, UK; Research Complex at Harwell, STFC Rutherford Appleton Laboratory, Harwell Campus, Didcot, UK)

Biomass offers a route to obtain chemical products normally derived from crude oil, from a more sustainable and carbon neutral source (since biomass absorbs  $\text{CO}_2$  for photosynthesis). The oxygen content of biomass, however, poses some problems, causing bio-oils to be more acidic and unstable than their crude oil derived counterparts. One method for the removal of oxygenates is through Catalytic Fast Pyrolysis of biomass (CFP), where biomass is pyrolyzed using fast heating rates and the resulting vapours are upgraded over zeolite catalysts.

Mechanistic studies are few in this area but some point towards the idea of a hydrocarbon pool mechanism, where hydrocarbons build up in zeolite pores to react with further pyrolysis vapours, undergoing decarbonylation, decarboxylation and dehydrogenation to produce aromatic species, olefins, CO and  $\text{CO}_2$ , as well as undesirable coke which builds up. During this upgrading process, zeolites deactivate rapidly through coking, making frequent regeneration necessary and affecting process efficiency. Through understanding these chemical transformations, we can gain insight as to how reaction efficiency can be improved.

Raman Spectroscopy is a useful tool for mechanistic studies, but in many cases catalyst defects or emissive hydrocarbon species present can cause intense

Contact: A.M. Beale ([andrew.beale@ucl.ac.uk](mailto:andrew.beale@ucl.ac.uk))

I. Sazanovich, M. Towrie (Central Laser Facility, Research Complex at Harwell, STFC Rutherford Appleton Laboratory, Harwell Campus, Didcot, UK)

M.J. Watson (Johnson Matthey PLC, Billingham, UK)

fluorescence, preventing Raman signals from being detected. To avoid fluorescence, UV or near-IR probe wavelengths can be used but these often result in sample damage and low signal intensity respectively. This work uses a visible wavelength source (400 nm) with a Kerr-gated spectrometer that allows Raman signals to be separated from fluorescence due to their different lifetimes.

In this work, we study the interaction of oxygenated hydrocarbons with zeolites by operando Kerr-gated Raman Spectroscopy and identify reaction intermediates whilst measuring catalytic activity through mass spectrometry (MS).

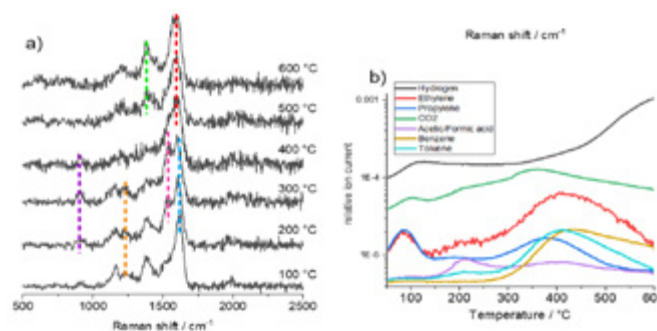


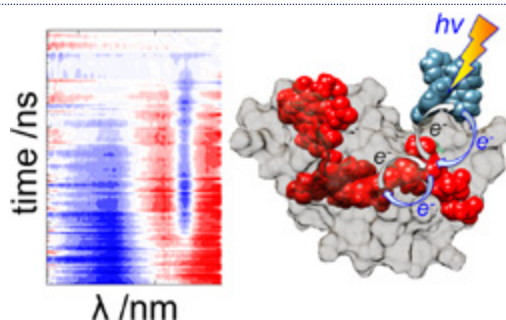
Figure a) Raman spectra collected during temperature ramp experiment of furan on H-ZSM-5 Si/Al 40 b) MS data simultaneously measured

## Ultrafast Light-Driven Electron Transfer in a Ru(II)tris(bipyridine)-Labeled Multiheme Cytochrome

J.H. van Wonderen, C.R. Hall, K. Adamczyk, I. Heisler, S.E. Piper, T.A. Clarke, N.J. Watmough, S.R. Meech, J.N. Butt (School of Chemistry and School of Biological Sciences, University of East Anglia, Norwich, UK)  
X. Jiang, A. Carof (Department of Physics and Astronomy and Thomas-Young Centre, University College London, UK)

I.V. Sazanovich, M. Towrie (Central Laser Facility, Research Complex at Harwell, STFC Rutherford Appleton Laboratory, Harwell Campus, Didcot, UK)  
J. Blumberger (Department of Physics and Astronomy and Thomas-Young Centre, University College London, UK; Institute for Advance Study, Technische Universität München, Garching, Germany)

Multiheme cytochromes attract much attention for their electron transport properties. These proteins conduct electrons across bacterial cell walls and along extracellular filaments and when purified can serve as bionanoelectronic junctions. Thus, it is important and necessary to identify and understand the factors governing electron transfer in this family of proteins. To this end we have used ultrafast transient absorbance spectroscopy, to define heme–heme electron transfer dynamics in the representative multiheme cytochrome STC from *Shewanella oneidensis* in aqueous solution. STC was photosensitized by site-selective labelling with a tris(bipyridine) Ru(II) dye and the dynamics of light-driven electron transfer described by a kinetic model corroborated by molecular dynamics simulation and density functional theory calculations. The results are significant in demonstrating the opportunities for pump–probe spectroscopies to resolve interheme electron transfer in Ru-labelled multiheme cytochromes.



Differential transient absorbance (left) for visible wavelengths (blue = positive features, red = negative features) following excitation of tris(bipyridine) Ru(II) attached to the STC protein (right).

Reproduced from J.H. van Wonderen et al. *J. Am. Chem. Soc.* 2019, 141, 38, 15190–15200, doi: 10.1021/jacs.9b06858, © 2019 American Chemical Society, under the terms of the Creative Commons Attribution 4.0 International License

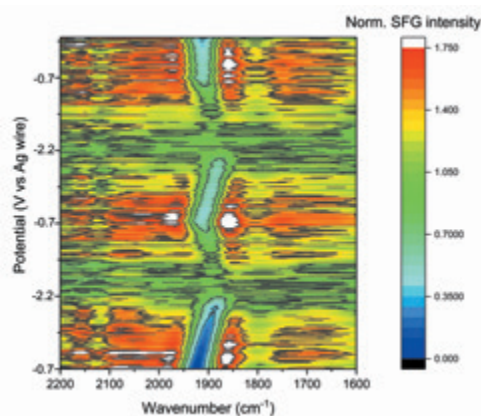
Contact: J.N. Butt (J.Butt@uea.ac.uk)

## Assessing the Viability of Heterodyne VSFG Spectroscopic Studies of Electrode Interfaces

A.M. Gardner, K.H. Saeed, A.J. Cowan (Stephenson Institute for Renewable Energy, University of Liverpool, UK)

P.M. Donaldson (Central Laser Facility, STFC Rutherford Appleton Laboratory, Harwell Campus, Didcot, UK)

Heterodyne vibrational sum frequency generation (HD-VSFG) spectroscopy allows for detection of molecules at surfaces, even at very low coverages, and yields both the phase and amplitude of SFG signal. Past application of HD-VSFG to the chemistry occurring at electrode surfaces is, however, limited. Here we report our efforts towards a broad-band HD-VSFG experiment for the study of CO<sub>2</sub> reduction electrocatalysis.



HD-VSFG spectra recorded as the potential of the Au working electrode is modulated between -0.7 and -2.2 V in the presence of [Mo(bpy)(CO)<sub>4</sub>] at 10 mV s<sup>-1</sup>.

Contact: A.J. Cowan (acowan@liverpool.ac.uk)

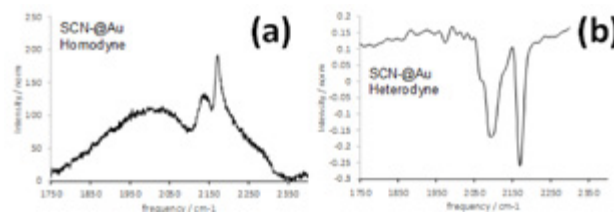
## Towards heterodyne detected IR-Visible Sum Frequency Generation at CLF-Ultra

G. Karras, C. Kirkbride, P.M. Donaldson (Central Laser Facility, STFC Rutherford Appleton Laboratory, Harwell Campus, Didcot, UK)

O. Al Bahri, J.M. Cole (Molecular Engineering Group, University of Cambridge, UK)  
K. Saeed, A.M. Gardner, A.C. Cowan (School of Physical Sciences, University of Liverpool, UK)

Surface specific IR-Visible Sum Frequency Generation (SFG) has the ability to measure vibrational spectra of monolayer level buried interfaces. The provision of IR-Visible SFG spectroscopy at CLF-Ultra has been driven by successful studies of catalysis at electrochemical interfaces. In this article we demonstrate progress towards measuring SFG spectra with heterodyne detection, which has the advantage of being background free and free from the artefacts associated with in-quadrature detection.

Contact: P.M. Donaldson (paul.donaldson@stfc.ac.uk)



A comparison of SCN- ions on a gold substrate measured with homodyne (a) and heterodyne (b) detected IR-Visible SFG spectroscopy. (a) was recorded with a 2 second accumulation of signal; (b) was recorded with a 20 second accumulation of signal. Heterodyne signal fringes were recovered from a spectrum recorded with a 4 ps delay between the local oscillator and the SFG signal.

## 2D-IR spectroscopy reveals multiple hydrogen bonded ensembles of the thiocyanate ion in the protic ionic liquid ethyl ammonium nitrate

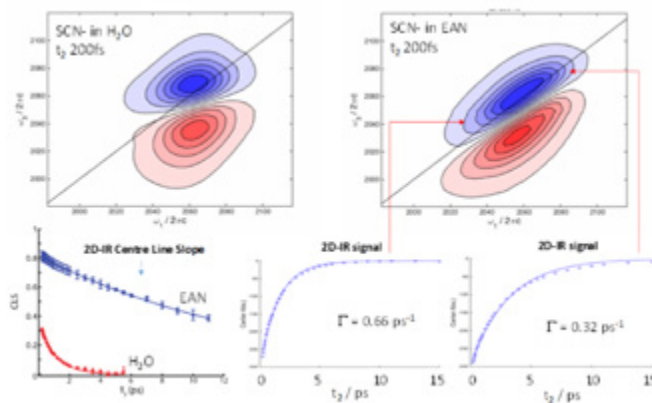
A.W. Parker, P.M. Donaldson (Central Laser Facility, STFC Rutherford Appleton Laboratory, Harwell Campus, Didcot, UK)

C. Johnson, S.G. Roe (Department of Chemistry, University of Pittsburgh, USA)

2D-IR spectroscopy can measure the ultrafast structural dynamics of solvated molecules in equilibrium. Here we are interested in the hydrogen bonding dynamics of the simplest protic ionic liquid – ethyl ammonium nitrate (EAN), which we study via the 2D-IR spectrum of a guest solute ion thiocyanate (SCN<sup>-</sup>). We bring together advances in both experiment and in data modelling/fitting to provide a most concise and quantitative measure of the hydrogen bond dynamics of SCN<sup>-</sup> in EAN.

We have applied polarization and temperature-dependent 2D-IR spectroscopy to quantify the ultrafast (<10 ps) hydrogen bond dynamics of a guest ion SCN<sup>-</sup> in the protic ionic liquid EAN. Not only did we learn quantitatively about the energetics and rates of hydrogen bonding in the two different ensembles observed, this type of measurement (a first for the Ultra facility) and the data analysis techniques used represent a powerful protocol for future studies of other electrolytes.

Contact: S.G. Roe (sgr@pitt.edu)  
P.M. Donaldson (paul.donaldson@stfc.ac.uk)



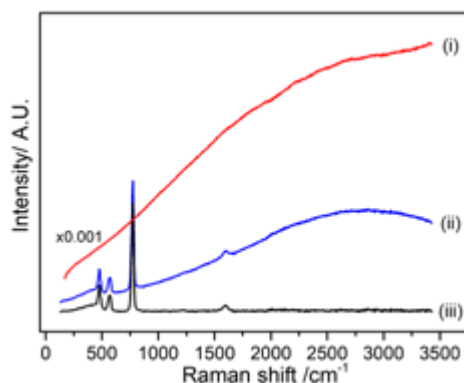
2D-IR spectroscopy reveals that the structural and vibrational dynamics of SCN<sup>-</sup> in protic ionic liquid EAN is significantly different from that of water

## Kerr gated Raman spectroscopy of $\text{LiPF}_6$ salt and $\text{LiPF}_6$ -based organic carbonate electrolyte for Li-ion batteries

**L. Cabo-Fernandez, A.R. Neale, F. Braga, L.J. Hardwick** (Stephenson Institute for Renewable Energy, Department of Chemistry, University of Liverpool, Peach Street, UK)  
**I.V. Sazanovich** (Central Laser Facility, Research Complex at Harwell, STFC Rutherford Appleton Laboratory, Harwell Campus, Didcot, UK)

**R. Kosteckí** (Energy Storage and Distributed Resources Division, Lawrence Berkeley National Laboratory, California, USA)

Fluorescent species are formed during cycling of lithium ion batteries as a result of electrolyte decomposition due to the instability of the non-aqueous electrolytes and side reactions that occur at the electrode surface. The increase in the background fluorescence due to the presence of these components makes it harder to analyse data due to the spectroscopic overlap of Raman scattering and fluorescence. Herein, Kerr gated Raman spectroscopy was shown to be an effective technique for the isolation of the scattering effect from the fluorescence enabling the collection of the Raman spectra of  $\text{LiPF}_6$  salt and  $\text{LiPF}_6$ -based organic carbonate electrolyte, without the interference of the fluorescence component. Kerr gated Raman was able to identify  $\text{POF}_3$  on the  $\text{LiPF}_6$  particle surface, after the addition of trace water.



Raman spectra of anhydrous  $\text{LiPF}_6$  measured with a 400 nm laser excitation in (i) CW mode and (ii) Kerr gated mode and (iii) the baseline corrected Kerr gated spectra. Intensity of (i) scaled by  $\times 0.001$  to view data on same axis.

Reproduced from *Phys. Chem. Chem. Phys.*, 2019, 21, 23833-23842, with permission from the Royal Society of Chemistry under the Creative Commons Attribution 3.0 Unported Licence.

Contact: L.J. Hardwick ([hardwick@liverpool.ac.uk](mailto:hardwick@liverpool.ac.uk))

## 2D-IR spectroelectrochemistry of singly oxidized $\text{cis}[\text{Ru}(4,4'-(\text{MeO})_2\text{-bpy})_2(\text{NCS})_2]^+$ and reduced $\text{cis}[\text{Ru}(4,4'-(\text{COOEt})_2\text{-bpy})_2(\text{NCS})_2]^+$ ( $\text{bpy} = 2,2'$ -bipyridine) complexes

**M. Piží, A. Viček** (Queen Mary University of London, School of Biological and Chemical Sciences, London, UK)  
**J.O. Taylor, F. Hartl** (Department of Chemistry, University of Reading, UK)

**P.M. Donaldson** (Central Laser Facility, Research Complex at Harwell, STFC Rutherford Appleton Laboratory, Harwell Campus, Didcot, UK)

Infra-red transmittance spectroelectrochemistry is now well-established as a go-to technique for investigating a host of different redox reactions. The enormous potential of this technique has yet to be fully realised. Proof-of-concept measurements supported by anharmonic-frequency quantum-chemical calculations have revealed the exciting potential of this technique in combination with pump-probe 2D-IR laser spectroscopy. Vibrational relaxation of the IR-active thiocyanate stretching modes in the two title reference complexes was investigated in their ground states as well as  $1e^-$  Ru-oxidized (for Ru-bis(dimethoxy)bpy) and  $1e^-$  bpy-reduced (for Ru-bis(ester)bpy) states. Dramatic shortening of the NCS-stretching vibrational relaxation was observed for the Ru-oxidized complex, comparable to the triplet Ru-to-bpy excited state of the same complex. On the other hand, the bis(ester)bpy-localized reduction has a negligible effect on the dynamics of the NCS-stretching vibration. An accurate analysis of the experimental data and understanding of the dynamic behaviour requires high-level DFT calculations of anharmonic vibrational energies and diagonal/off-diagonal anharmonicity. The results will have an important impact on the description of relaxation processes in photoinduced electron-transfer reactions and their role in photo-redox catalysis.

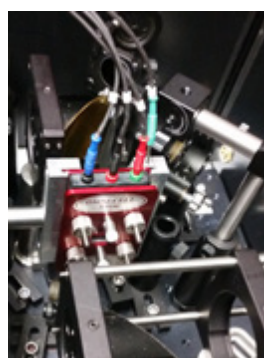


Figure 1: LIFETIME-OTTLE cell setup used for the 2D-IR spectroelectrochemical experiments

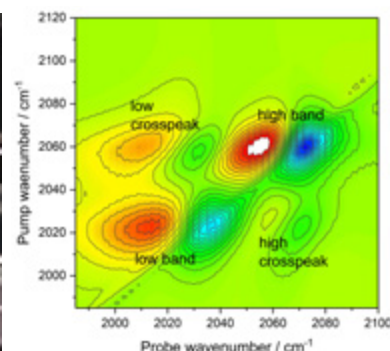


Figure 2: Representative 2D-IR spectrum of in situ generated  $\text{cis}[\text{Ru}(4,4'-(\text{MeO})_2\text{-bpy})_2(\text{NCS})_2]^+$  in DMF

Contact: F. Hartl ([f.hartl@reading.ac.uk](mailto:f.hartl@reading.ac.uk))

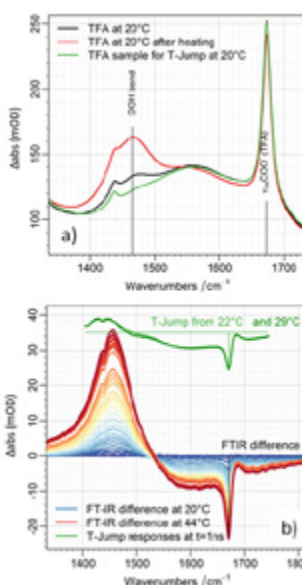
## Temperature-Jump Time Resolved Infrared Spectroscopy of Trifluoroacetic Acid Solutions – Characterising the T-Jump

R. Fritsch, L. Minnes (Department of Physics, University of Strathclyde, Glasgow, UK)  
 G.M. Greetham, I.P. Clark, M. Towrie, A.W. Parker (Central Laser Facility, STFC Rutherford  
 Appleton Laboratory, Harwell Campus, Didcot, UK)

D. J. Shaw, N.T. Hunt (Department of Chemistry, University of York, York, UK)

There is an increasing appreciation of the involvement of dynamic structural changes in biological function, from the unwinding of double stranded DNA to structural changes of proteins during their biological mechanisms. The molecular details of these transitions are of significant interest, and the ability to measure them in real time would provide valuable experimental insight. Temperature jump time-resolved spectroscopy, in which a nanosecond duration infrared laser pulse tuned to solvent absorptions induces a rapid rise in temperature, has become a powerful method for studying biomolecular transitions. It is, however, important to carefully calibrate the temperature jump achieved in order to separate biomolecular dynamics from those of the solvent bath. In this report, we describe the use of trifluoroacetic acid solutions to characterise the magnitude and dynamics of a temperature jump initiated using a high repetition rate pumping and time resolved multiple probe infrared detection methodology.

Contact: N.T. Hunt (neil.hunt@york.ac.uk)



a) IR absorption spectra of TFA in  $D_2O$  solution (black and red). NB the increase in absorbance of the HOD bending vibrational mode after heating due to further exchange with the environment. Green shows the absorption spectrum of the sample used to acquire the data in b).

b) Temperature-dependent IR absorption difference spectra of TFA (lower). Colour scale runs from 20°C (blue) to 44°C (red). The difference spectra are relative to the spectrum at 20°C. Green traces show T-jump-IR spectra of the same sample obtained at a T-jump-probe delay time of 1 ns.

## Evaluation of Ultra A for the detection and analysis of drug-target structural changes using EVV 2DIR spectroscopy

D.R. Klug (Department of Chemistry, Imperial College London, UK)

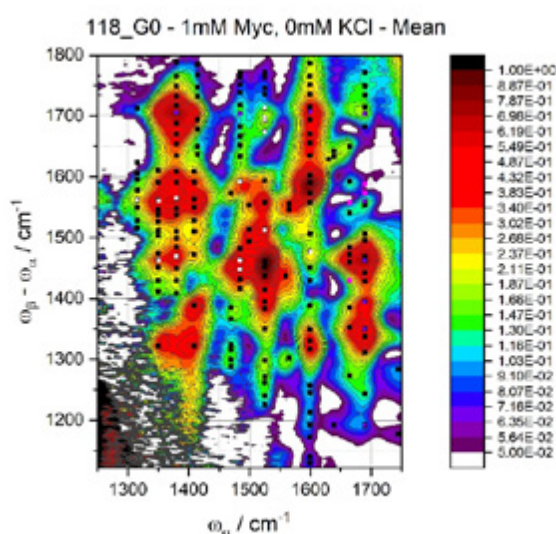
When two molecules come together to form a complex, part of the interaction is the coupling of molecular vibrations that originated on the unbound molecular species. Previous research has shown that the new couplings can be detected by EVV 2DIR spectroscopy[1]. However, despite the power of existing structural biology methods, many limitations remain such that structural data is not available in sufficient quantity or quality to drive particular drug-discovery/development strategies.

The limiting factor in our studies of drug-target binding has been the signal to noise and reproducibility achievable by the spectroscopic apparatus. In collaboration with the CLF, we ported our EVV experiment onto CLF apparatus. This was successfully completed and showed that EVV 2DIR experiments could be successfully performed on both Ultra A and LifeTIME.

Following this knowledge transfer activity, we explored the utility of the new apparatus against drug-kinase binding, and the ability of EVV 2DIR spectroscopy to be used to assign structural features to G-quadruplex DNA.

Modifications to the Ultra A-EVV 2DIR setup have been identified which have the potential to improve the signal to noise and reproducibility of the data, and make the system comparable or superior to the performance of the obsolete Imperial College system.

[1] Guo, R. et al., *Phys. Chem. Chem. Phys.* 11(38): 8417-8421, 2009



EVV 2DIR spectrum of Myc2345 in the absence of potassium ions taken using Ultra A. Over 170 individual peaks are identifiable.

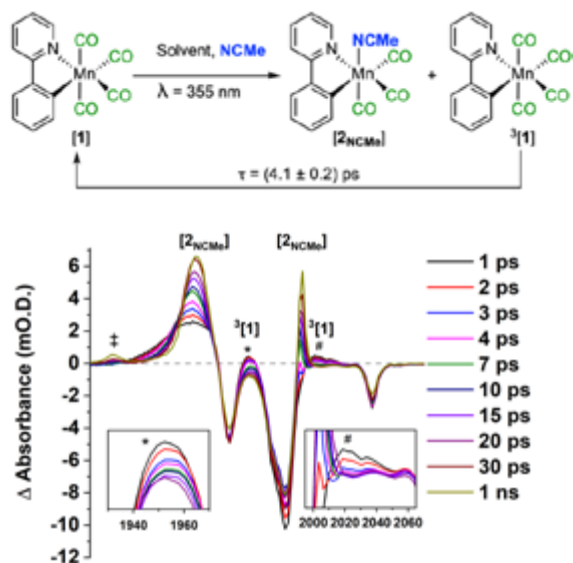
Contact: D. Klug (d.klug@imperial.ac.uk)

## Time-resolved Infra-red Spectroscopy Provides Insight into the Solvation of Unsaturated Transition Metal Complexes

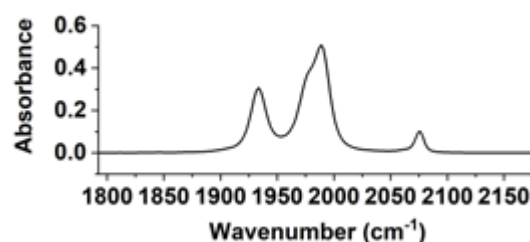
B.J. Aucott, L.A. Hammarback, B.E. Moulton, A.K. Duhme-Klair, I.J.S. Fairlamb, J.M. Lynam  
(Department of Chemistry, University of York, UK)

I.P. Clark, I.V. Sazanovich, M. Towrie (Central Laser Facility, STFC Rutherford Appleton Laboratory, Harwell Campus, Didcot, UK)

Photolysis of  $[\text{Mn}(\text{ppy})(\text{CO})_4][1]$  (ppy = 2-phenylpyridine) results in ultrafast ( $< 1$  ps) dissociation of a carbonyl ligand and formation of complexes  $\text{fac-}[\text{Mn}(\text{ppy})(\text{CO})_3(\text{S})]$  where S is the solvent medium employed. The nature of the complexes, and in particular the binding mode of the solvent, was probed by time-resolved multiple-probe spectroscopy (TR<sup>M</sup>PS). It was found that the solvation process is kinetically controlled, for



example, when ether solvents such as THF are employed, initial binding to the metal occurs through a C-H bond in a  $\sigma$ -type interaction. Subsequent isomerisation to the more thermodynamically stable oxygen-bound isomer then occurs over the course of ca. 20 ps. These data provide insight into solvation processes which are relevant to a number of reaction steps that underpin catalysis.



Top left: Scheme showing the reaction pathway.

Bottom left: TRIR spectra showing the formation of  $[2_{\text{NCMe}}]$  and  $^3[\text{Mn}(\text{ppy})(\text{CO})_4]$ .

Right: Ground state spectrum of  $[1]$  in NCMe.

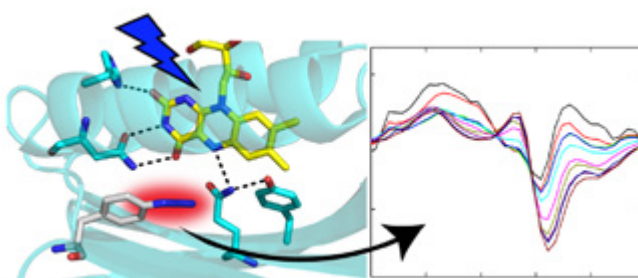
Contact: I.P. Clark ([ian.p.clark@stfc.ac.uk](mailto:ian.p.clark@stfc.ac.uk))

## Site-Specific Protein Dynamics Probed by Ultrafast Infrared Spectroscopy of a Noncanonical Amino Acid

C.R. Hall, K. Adamczyk, S.R. Meech (School of Chemistry, University of East Anglia, Norwich, UK)  
J. Tolentino Collado, J.N. Iuliano, A.A. Gil, P.J. Tonge (Department of Chemistry, Stony Brook University, New York, USA)

A. Lukacs (Department of Biophysics, Medical School, University of Pecs, Hungary)  
G.M. Greetham, I.V. Sazanovich (Central Laser Facility, STFC Rutherford Appleton Laboratory, Harwell Campus, Didcot, UK)

Real-time observation of structure changes associated with protein function remains a major challenge. Ultrafast pump-probe methods record dynamics in light activated proteins, but the assignment of spectroscopic observables to specific structure changes can be difficult. The BLUF (blue light using flavin) domain proteins are an important class of light sensing flavoprotein. Here, we incorporate the unnatural amino acid (UAA) azidophenylalanine (AzPhe) at key positions in the H-bonding environment of the isoalloxazine chromophore of two BLUF domains, namely, PixD and AppABLUF; both proteins retain the red-shift on irradiation characteristic of photoactivity. Steady state and ultrafast time resolved infrared difference measurements of the azido mode reveal site-specific information on the nature and dynamics of light driven structure change. AzPhe dynamics are thus shown to be an effective probe of BLUF domain photoactivation, revealing significant differences between the two proteins and a differential response of the two sites to chromophore excitation.



Reprinted with permission from Hall CR, Tolentino Collado J, Iuliano JN, et al. Site-Specific Protein Dynamics Probed by Ultrafast Infrared Spectroscopy of a Noncanonical Amino Acid. *J Phys Chem B*. 2019;123(45):9592-9597. doi:10.1021/acs.jpcc.9b09425. Copyright 2019 American Chemical Society.

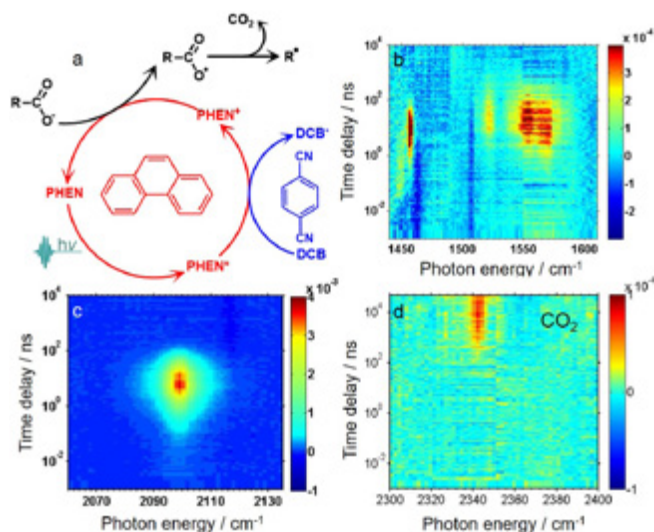
Contact: S.R. Meech ([s.meech@uea.ac.uk](mailto:s.meech@uea.ac.uk))

## Picosecond to millisecond tracking of a photocatalytic decarboxylation reaction provides direct mechanistic insights

A. Bhattacharjee (School of Chemistry, University of Bristol, UK; AMOLF, Amsterdam, The Netherlands)

M. Sneha, L. Lewis-Borrell, O. Tau, A. Orr-Ewing (School of Chemistry, University of Bristol, UK)  
I.P. Clark (Central Laser Facility, STFC Rutherford Appleton Laboratory, Harwell Campus, Didcot, UK)

The photochemical decarboxylation of carboxylic acids is a versatile route to free radical intermediates for chemical synthesis. However, the sequential nature of this multi-step reaction renders the mechanism challenging to probe. Here, we employ a 100 kHz mid-infrared probe in a transient absorption spectroscopy experiment to track the decarboxylation of cyclohexanecarboxylic acid in acetonitrile- $d_3$  over picosecond to millisecond timescales using a photooxidant pair (phenanthrene and 1,4-dicyanobenzene). Selective excitation of phenanthrene at 256 nm enables a diffusion-limited photoinduced electron transfer to 1,4-dicyanobenzene. A measured time offset in the rise of the  $CO_2$  byproduct reports on the lifetime ( $520 \pm 120$  ns) of a reactive carboxyl radical in solution, and spectroscopic observation of the carboxyl radical confirm its formation as a reaction intermediate. Precise clocking of the lifetimes of radicals generated in situ by an activated C-C bond fission will pave the way for improving the photocatalytic selectivity and turnover.



Photoredox cycle converting deprotonated carboxylic acids to reactive radicals (a), and the time-dependence of IR bands of (b)  $PHEN^+$ , (c)  $DCB^+$ , and (d)  $CO_2$  products

Reproduced from Bhattacharjee, A., Sneha, M., Lewis-Borrell, L. et al. *Nat Commun* 10, 5152 (2019), under the terms of the Creative Commons Attribution 4.0 International License. doi: 10.1038/s41467-019-13154-w

Contact: A. Orr-Ewing (a.orr-ewing@bristol.ac.uk)

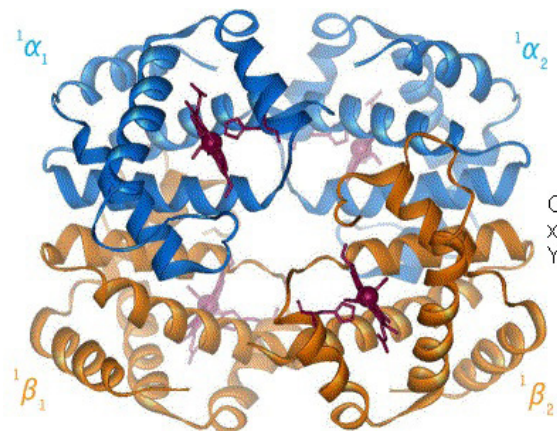
## Time-Resolved Multiple-Probe Infrared Spectroscopy Studies of Carbon Monoxide Migration through Internal Cavities in Haemoglobin

M.V. Parkhats, B.M. Dzhangarov, S.V. Lepeshkevich (B.I. Stepanov Institute of Physics, National Academy of Sciences of Belarus, Minsk, Belarus)

I.V. Sazanovich (Central Laser Facility, STFC Rutherford Appleton Laboratory, Harwell Campus, Didcot, UK)

S. N. Gilevich (Institute of Bioorganic Chemistry, National Academy of Sciences of Belarus, Minsk, Belarus)

Human haemoglobin reactivity towards ligands such as  $O_2$  and CO as well as ligand migration via the protein matrix is modulated by internal cavities. In the present work, a time-resolved multiple-probe picosecond to millisecond infrared technique developed at Ultra Facility was applied to determine the dynamics of the ligand migration via the internal cavities of haemoglobin. We studied both native haemoglobin (see figure) and its isolated  $\alpha$  and  $\beta$  chains. We succeeded in following the evolution of photodissociated CO ligand inside the protein matrix during geminate recombination. Moreover, we managed to detect the photodissociated CO molecules escaped from the protein into external media.



The schematic structure of human haemoglobin in Oxy state with  $\alpha$  and  $\beta$  subunits colour-coded.

Contact: I.V. Sazanovich (igor.sazanovich@stfc.ac.uk)